The resultant values of the internal heat- and mass-transfer coefficients may be used for calculating the temperature and humidity fields in objects made of lightweight aggregate concrete of the compositions under consideration during heat treatment in chambers with thermally insulating surfaces and also for selecting the optimum modes of treatment.

NOTATION

T, U, dimensionless temperature and moisture content; Fo, homochronicity number; N, dimensionless coordinate; εKo, Kossovich complex; Ly, inertial Lykov simplex; Pn, thermal gradient Posnov number; a, thermal diffusivity, m^2/h; b, distance between end points of measurement, m; Z_a, ξ_a, Z_p, arguments of the characteristic functions of irreversible thermodynamic processes; $t(x, \tau)$, $u(x, \tau)$, temperature and moisture content at the point with coordinate x at the instant of time τ; h, height of the sample, m; a_m, moisture-diffusion coefficient, m^2/h; δ, thermal gradient coefficient, 1/°C.

LITERATURE CITED

1. S. K. Bud'ko and M. T. Soldatkin, Beton i Zhelezobeton, No. 2 (1970).
2. A. V. Lykov, Transfer Phenomena in Capillary-Porous Solids [in Russian], GITTL, Moscow (1954).
3. A. G. Temkin, Study of Transient Heat and Mass Transfer [in Russian], Minsk (1966).
4. A. G. Temkin and D. I. Shtakel'berg, in: Thermal Conductivity and Diffusion [in Russian], Izd. Riga Politekh. Inst., Riga (1969).
5. V. P. Demidovich and I. A. Maron, Fundamentals of Computing Mathematics [in Russian], FM (1963).
6. I. B. Zasedatelev and G. V. Mishin, Beton i Zhelezobeton, No. 10 (1969).
7. L. A. Malinina and P. N. Gamayunov, Beton i Zhelezobeton, No. 8 (1971).
8. L. Ya. Volosyan and V. P. Zhuravleva, Inzh.-Fiz. Zh., 16, No. 10 (1969).

COMPUTATION OF A LAMINAR NON-SELF-SIMILAR SEMIBOUNDED FLUID JET

K. E. Dzhaugashtin and A. L. Yarin

UDC 532.522.2

The numerical solution of dynamic and heat problems of a laminar plane incompressible fluid jet being propagated along a solid surface is performed within the framework of boundary-layer theory.

§1. Dynamic and thermal problems on the propagation of a laminar, plane, near-wall fluid jet have been solved earlier on the basis of an asymptotic boundary-layer scheme in a self-similar formulation [1]. A method and results of a computation of a semiinfinite incompressible fluid jet in the whole flow domain are elucidated below.

The initial system of equations of motion and heat propagation of a plane stationary incompressible fluid boundary layer is presented on the left in Table 1. The equations and initial and boundary conditions are written in dimensionless form, where the bar above the dimensionless quantities has been omitted for simplicity.

It is assumed that the jet issues from a slot with uniform velocity and temperature profiles in parallel to the surface of a solid wall. At a range of one integration spacing along the transverse coordinate, the magnitude of the velocity at the wall and at the outer edge of the slot drops to zero at the exit and the temperature becomes equal to the value of the

Translated from Inzhenerno-Fizicheskii Zhurnal, Vol. 32, No. 4, pp. 666-673, April, 1977. Original article submitted March 26, 1976.

TABLE 1. System of Equations and Boundary Conditions

x, y		ξ, η
$u\frac{\partial u}{\partial x}+v\frac{\partial u}{\partial y}=\frac{\partial^2 u}{\partial y^2}$ $\frac{\partial u}{\partial x}+\frac{\partial v}{\partial y}=0$	(1)	$\frac{\partial u}{\partial \xi}=\frac{3}{2}u^2\frac{\partial u}{\partial \eta}+\psi^2u^2\frac{\partial}{\partial \eta}\left(u\frac{\partial u}{\partial \eta}\right)$ $\psi=\left(2\int_0^\eta \frac{1}{u}\,d\eta\right)^{1/2}$
$u=1$ for $0<y<1$ $u=0$ for $y=0,\ 1\leqslant y<\infty$ } $x=0$ $u=0$ for $y=0$ $u=0$ for $y=\infty$ } $x>0$		$u=1$ for $0<\eta<\frac{1}{2}$ $u=0$ for $\eta=0,\ \eta=\frac{1}{2}$ } $\xi=0$ $u=0$ $\psi=0$ for $\eta=0$ $u=0$ for $\eta=\frac{1}{2}$ } $\xi>0$
$u\frac{\partial \Delta T}{\partial x}+v\frac{\partial \Delta T}{\partial y}=\frac{1}{\sigma}\frac{\partial^2 \Delta T}{\partial y^2}$	(2)	$\frac{\partial \Delta T}{\partial \xi}=\frac{\psi u}{\sigma}\frac{\partial}{\partial \eta}\left(\psi u^2\frac{\partial \Delta T}{\partial \eta}\right)-$ $-\left(\psi^2u^2\frac{\partial u}{\partial \eta}-\frac{u^2}{2}\right)\frac{\partial \Delta T}{\partial \eta}$
$\Delta T=1$ for $0<y<1$ $\Delta T=0$ for $y=0, 1\leqslant y<\infty$ } $x=0$ $\Delta T=0$ for $y=0$ $\Delta T=0$ for $y=\infty$ } $x>0$	A	$\Delta T=1$ for $0<\eta<\frac{1}{2}$ $\Delta T=0$ for $\eta=0,\ \eta=\frac{1}{2}$ } $\xi=0$ $\Delta T=0$ for $\eta=0$ $\Delta T=0$ for $\eta=\frac{1}{2}$ } $\xi>0$
$\Delta T=1$ for $0\leqslant y<1$ $\Delta T=0$ for $1\leqslant y<\infty$ } $x=0$ $\frac{\partial \Delta T}{\partial y}=0$ for $y=0$ $\Delta T=0$ for $y=\infty$ } $x>0$	B	$\Delta T=1$ for $0\leqslant\eta<\frac{1}{2}$ $\Delta T=0$ for $\eta=\frac{1}{2}$ } $\xi=0$ $\frac{\partial \Delta T}{\partial \eta}=-\infty$ for $\eta=0$ $\Delta T=0$ for $\eta=\frac{1}{2}$ } $\xi>0$
$\Delta T=1$ for $y=0$ $\Delta T=C$ for $0<y<1$ $\Delta T=0$ for $1\leqslant y<\infty$ } $x=0$ $\Delta T=1$ for $y=0$ $\Delta T=0$ for $y=\infty$ } $x>0$	C	$\Delta T=1$ for $\eta=0$ $\Delta T=C$ for $0<\eta<\frac{1}{2}$ $\Delta T=0$ for $\eta=\frac{1}{2}$ } $\xi=0$ $\Delta T=1$ for $\eta=0$ $\Delta T=0$ for $\eta=\frac{1}{2}$ } $\xi>0$

temperature at the wall and in the external medium, respectively. The temperature of the external environment is assumed constant. Three kinds of boundary conditions at the wall will be examined below: A) The magnitudes of the temperatures at the wall and in the quiescent medium are identical; B) a non-heat-conductive wall; C) the wall temperature is fixed and different from the temperature of the environment [see Table 1 with the appropriate sections (2); A, B, C].

By analogy with [2], let us introduce a change of variable

$$\xi=x,\quad \eta=\int_0^y \psi u^2 dy, \tag{3}$$

which assures automatic compliance with the integral conservation condition for semiinfinite jets in the numerical solution

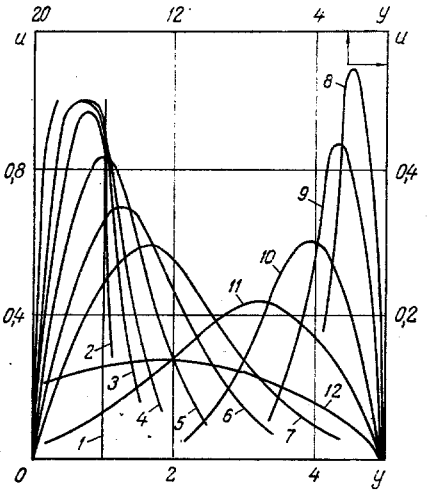

Fig. 1

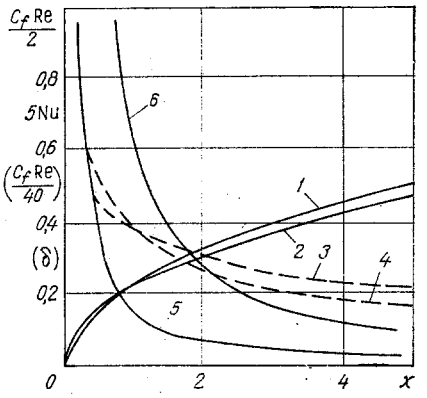

Fig. 2

Fig. 1. Longitudinal velocity component profiles at different sections of the jet: 1) x = 0; 2) 0.0017; 3) 0.011; 4) 0.029; 5) 0.071; 6) 0.140; 7) 0.229; 8) 0.268; 9) 0.461; 10) 1.031; 11) 2.196; 12) 4.574.

Fig. 2. Change in the friction coefficient, boundary-layer thickness, and Nusselt number along the wall (case A, σ = 0.72). Comparison with the Blasius solution in the initial section: 1) $\delta = 5\sqrt{x}$; 2) δ in a semiinfinite jet; 3) $C_f Re/2$ for a semiinfinite jet; 4) $C_f Re/2 = 0.332/\sqrt{x}$ (notation of the coordinate axes in cases 1-4 is presented in parentheses); 5) $1 - (C_f Re/2)$; 6) Nu.

$$\int_0^\infty \psi u^2 dy = E = \text{const} \tag{4}$$

and converts the infinite range of integration into a strip of finite width for the numerical solution of the equations.

The equations of motion and heat propagation, and the initial and boundary conditions, in the new variables take the form indicated on the right in the table. Hence, the transverse velocity component is determined by means of the formula

$$v = u\frac{\partial y}{\partial \xi} + \int_0^\eta \frac{1}{\psi^2 u^2}\frac{\partial}{\partial \xi}(\psi u)\, d\eta. \tag{5}$$

The passage to the physical plane is realized by the reciprocal replacement

$$x = \xi, \quad y = \int_0^\eta \frac{1}{\psi u^2}\, d\eta. \tag{6}$$

Equations (1) and (2) with the appropriate initial and boundary conditions were solved by the method of lines in the half-strip $\eta \in [0, 1/2]$, $\xi \geq 0$ [the width of the half-strip is related to the condition that $\eta(\infty) = \int_0^\infty \psi u^2\, dy = \frac{1}{2}$) for the uniform initial velocity profile]. The derivatives with respect to η in the initial equations were approximated by nonsymmetric differences [3] on each of the lines $\eta = \eta_k$ (k = 1, 2, ..., n). This was caused by the need to select a sufficiently small spacing in the variable η near the boundary of the half-strip, where the values of the velocity and temperature gradients are a maximum [4]. The value n = 39 was taken in the computations; the spacing in η varied from $\Delta\eta = 0.267 \cdot 10^{-2}$ near the half-strip boundary to $\Delta\eta = 0.187 \cdot 10^{-1}$ at the center. The system of ordinary differential equations corresponding to the initial equations of motion and heat propagation was integrated by the Runge—Kutta method with automatic selection of the spacing in ξ. Integration was performed to the accuracy of four decimals.

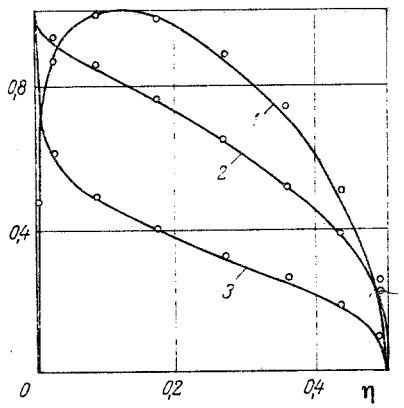

Fig. 3

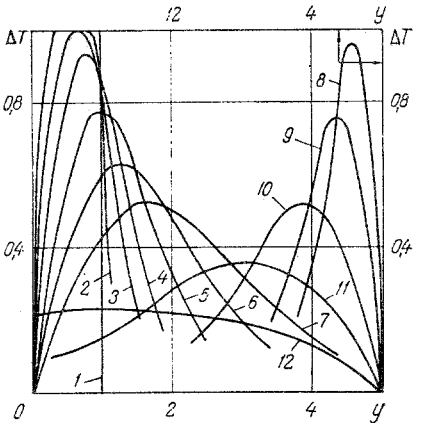

Fig. 4

Fig. 3. Comparison between numerical computations of the velocity and temperature profiles in the self-similar domain (points) and the self-similar solutions (solid lines): 1) u/u_{max}; 2) $\Delta T/\Delta T_w$ (case B, $\sigma = 0.72$); 3) ΔT (case C, $\sigma = 0.72$).

Fig. 4. Temperature profiles (case A, $\sigma = 0.72$); the notation for the sections along the longitudinal coordinate is the same as in Fig. 1.

The numerical solution of the system of equations is fraught with definite difficulties. One is the singularity associated with the second equation of (1) or its equivalent:

$$u\frac{\partial\psi^2}{\partial\eta} = 2. \tag{7}$$

For $\eta = 0$ the value of $\partial\psi^2/\partial\eta$ becomes infinite, which excludes the possibility of using (7) near the wall. Hence, an approximate relationship for (7) was obtained for the computations. To derive it, let us multiply (7) by u and let us integrate with respect to η:

$$\psi^2u^2 = 2\int_0^\eta\left(u + \psi^2u\frac{\partial u}{\partial\eta}\right)d\eta. \tag{8}$$

Let us evaluate the integral by the trapezoid formula for $\eta = \eta_1$ with the boundary conditions (1) taken into account:

$$\psi_1^2u_1^2 = \left\{\left[u_1 + \left(\psi^2u\frac{\partial u}{\partial\eta}\right)_{\eta=\eta_1}\right] + \left(\psi^2u\frac{\partial u}{\partial\eta}\right)_{\eta=0}\right\}\eta_1. \tag{9}$$

Let us show that the last term on the right side is identically zero. Indeed, it follows from the power series expansion of the velocity profile in y with the contour relations taken into account that $u \sim y$ in the physical plane, while $u \sim \eta^{1/5}$ in the new variables. Using this and expanding the indeterminacy in the expression in the last member in (9), we obtain

$$\left(\psi^2u\frac{\partial u}{\partial\eta}\right)_{\eta=0} \sim \eta^{1/5}|_{\eta=0} \equiv 0. \tag{10}$$

Hence, from (9) we find the following approximate formula to evaluate ψ_1:

$$\psi_1^2 = \frac{\eta_1}{u_1 - \eta_1\left(\frac{\partial u}{\partial\eta}\right)_1}. \tag{11}$$

It should be noted that a series expansion of the velocity profile in the transverse coordinate (analogously to the case B in the thermal problem) was also used to approximate (7). Hence, it turns out that the velocity and temperature profiles at $\sigma \leq 1$ differ insignificantly from those computed on the basis of the approximation (11). However, at $\sigma > 1$ a break (physically showing the inaccuracy of the approximation) appears in the temperature profiles near the wall, which is retained in the whole temperature range. The break is considerably less

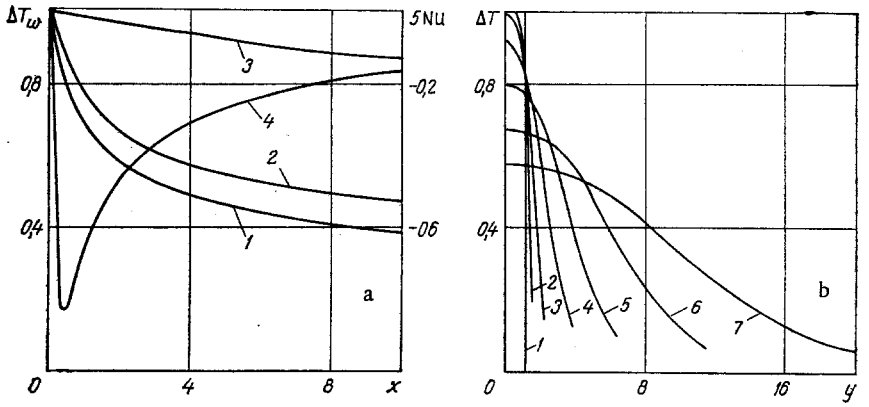

Fig. 5. Results of computing the temperature field: a) change in wall temperature (case B): 1) $\sigma = 0.72$; 2) 1; 3) 2; 4) Nusselt number (case C, $\sigma = 0.72$); b) temperature profiles (case B, $\sigma = 0.72$) at different jet sections: 1) x = 0; 2) 0.0079; 3) 0.048; 4) 0.184; 5) 0.461; 6) 1.031; 7) 2.196.

definite when using (11) and vanishes rapidly with distance from the initial section. Hence, computations performed on the basis of the approximation (11) will henceforth be presented, but they are nevertheless bounded by the value $\sigma \leq 1$ (mainly $\sigma = 0.72$). It follows from the above that computations of the temperature field for $\sigma > 1$ can be used to estimate the suitability of any scheme to compute the dynamic problem. In the physical plane this is associated with the fact that the predominant part in heat transport belongs to convection for $\sigma > 1$, and hence the inaccuracy in the computational scheme for the velocity field can be reduced to a qualitative distinction between the computed and the real temperature fields.

The singularity associated with the velocity and stream function vanishing at the wall occurs during execution of the reciprocal transformation $\eta \to y$ (6). However, the equivalent expression (3) can be used for the computations; by evaluating the integral by the trapezoid formula we obtain $y_1 = 2\eta_1/\psi_1 u_1^2$.

Now let us examine the boundary condition for the temperature field on a heat-insulated wall (case B). The temperature gradients in the x, y and ξ, η coordinates are connected by the relationship

$$\psi u^2 \left.\frac{\partial \Delta T}{\partial \eta}\right|_{\eta=0} = \left.\frac{\partial \Delta T}{\partial y}\right|_{y=0}, \tag{12}$$

where by assumption $\partial \Delta T/\partial y|_{y=0}$. Using the heat-propagation equation and expanding the indeterminacy twice, we can see that

$$\left.\frac{\partial \Delta T}{\partial \eta}\right|_{\eta=0} = -\infty. \tag{13}$$

To realize this condition in the numerical solution, let us use a series expansion of the temperature in powers of y: $\Delta T = \Delta T_w - a_1 y^3$, from which it follows that the temperature for small η varies in the new variables according to the law

$$\Delta T = \Delta T_w - a\eta^{3/5} \tag{14}$$

(ΔT_w, a, and a_1 are functions of ξ). Writing the value of the temperature near the wall on the first and second lines

$$\Delta T_1 = \Delta T_w - a\eta_1^{3/5}, \quad \Delta T_2 = \Delta T_w - a\eta_2^{3/5}, \tag{15}$$

we find an expression for

$$\Delta T_w = \frac{\Delta T_1 - \left(\frac{\eta_1}{\eta_2}\right)^{3/5} \Delta T_2}{1 - \left(\frac{\eta_1}{\eta_2}\right)^{3/5}}. \tag{16}$$

The value of the wall temperature (16) is the boundary condition for the thermal problem in case B in place of (13).

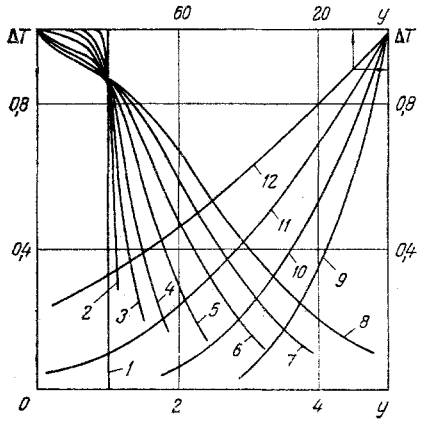

Fig. 6. Temperature profiles at different jet sections (case C, $\sigma = 0.72$): 1) $x = 0$; 2) 0.0017; 3) 0.011; 4) 0.029; 5) 0.063; 6) 0.127; 7) 0.183; 8) 0.267; 9) 5.844; 10) 10.599; 11) 19.477; 12) 39.724.

§2. The results of a numerical computation of the dynamic problem (Fig. 1) show that the flow domain of a semiinfinite jet can provisionally be separated into three sections. For the first (the initial section $0 \leq \xi \lesssim 0.015$), the escape velocity from the nozzle is conserved within the limits of a certain zone which vanishes at the end of the section. Hence, the external jet domain is developed as a mixing layer and the internal domain, as a near-wall boundary layer (Fig. 1). A comparison between the regularities of internal jet domain development in the initial section and the Blasius solution for a plate is shown in Fig. 2. Let us note that since the Blasius solution for a plate can be used at ranges from the leading edge which considerably exceed the viscous length, the comparison presented is suitable for sufficiently large Reynolds numbers. It is seen that the values of the boundary-layer thickness (the distance from the wall at which the velocity u differs by 0.01 from the external stream velocity is taken as the boundary-layer thickness) and the drag coefficient $[C_f = 2(\tau_w/\rho U^2) = (2/\mathrm{Re})(\partial u/\partial y)\big|_{y=0}]$ are close.

Rearrangement of the flow field, which terminates (for $\xi \simeq 4$) by emergence into the self-similar mode, occurs in the transition region. The latter is shown by a comparison between the numerical and self-similar solution (Fig. 3):

$$u = \frac{\sqrt{10E}}{3}\,\frac{1}{\sqrt{\xi}}\,z^{\frac{1}{2}}\left(1 - z^{\frac{3}{2}}\right), \quad \eta = \frac{E}{3}\,z^{-\frac{5}{2}}\left(8 - 5z^{\frac{3}{2}}\right). \tag{17}$$

It is seen from Fig. 2 that the drag coefficient diminishes comparatively rapidly in the initial section.

The temperature field for the boundary conditions A (Fig. 4) is deformed qualitatively, as is the velocity field. The change in the Nusselt number $\mathrm{Nu} = q_w d/(T_0 - T_\infty) = \partial\Delta T/\partial y\big|_{y=0}$ along the wall corresponds approximately to the Reynolds analogy (Fig. 2, curve 6). The self-similar temperature profile under boundary conditions of the type A will exist only for $\sigma = 1$ and has the form

$$\Delta T = \frac{k}{E}\,u \qquad \left(k = \int_0^\infty \psi u \Delta T\, dy\right). \tag{18}$$

The wall temperature for a flow along a heat-insulated wall will diminish with distance from the initial section (Fig. 5). The wall temperature increases with increase of the Prandtl number. The length of the thermal stabilization section ($\xi \simeq 2$ for $\sigma = 0.72$) is less than the dynamic length. The increase of the Prandtl number increases the thermal stabilization length. The self-similar temperature profile has the form (Fig. 3)

$$\Delta T = \frac{Q}{(40E)^{1/4}}\,\frac{1}{\xi^{1/4}}\,\frac{(1 - z^{3/2})^\sigma}{\int_0^1 (1 - z^{3/2})^\sigma\, dz}, \qquad Q = \int_0^\infty \Delta T u\, dy. \tag{19}$$

Complex rearrangement of the temperature field from the jet value in the initial section to a distribution characteristic for the boundary layer at a constant wall temperature occurs under the boundary conditions C. The significant length in the thermal stabilization section ($\xi \simeq 20$ for $C = 1$) and the nature of the change in Nusselt number $\mathrm{Nu} = q_w d/(T_w - T_\infty) = \partial\Delta T/\partial y\big|_{y=0}$ over the longitudinal coordinate x (Fig. 5a) is also visibly associated with this circumstance. This dependence has a minimum at some distance from the jet initial section.

The temperature profiles at different jet sections in the initial and transition regions are represented in Fig. 6. A comparison between the self-similar temperature profile obtained numerically and the self-similar solution of the heat-propagation equation (Fig. 3)

$$\Delta T = 1 - \frac{\int_0^z z^{-\frac{1}{2}} (1 - z^{3/2})^{\sigma-1} dz}{\int_0^1 z^{-\frac{1}{2}} (1 - z^{3/2})^{\sigma-1} dz} \qquad (20)$$

indicates the agreement between these solutions over the whole jet cross section.

NOTATION

d, slot width; U, fluid velocity at the exit from the slot; ν, coefficient of kinematic fluid velocity; σ, Prandtl number; $Re = Ud/\nu$, Reynolds number; T, temperature; T_0, T_∞, T_W, values of the temperature at the slot exit, the quiescent medium, and the wall, respectively; $\bar{x} = x/dRe$, $\bar{y} = y/d$, dimensionless longitudinal and transverse coordinates; $\bar{u} = u/U$, $\bar{v} = (v/U) \cdot Re$, dimensionless longitudinal and transverse velocities; u_{max}, maximum velocity in the jet cross section; $\Delta T_1 = T_0 - T_\infty$ for cases A and B; $\Delta T_1 = T_W - T_\infty$ for case C; $\overline{\Delta T} = (T - T_\infty)/\Delta T_1$, excess temperature; q, heat or thermal flux; $\bar{\psi}$, stream function ($\bar{u} = \partial\bar{\psi}/\partial\bar{y}$); $\bar{\delta} = \delta/d$, dimensionless boundary-layer thickness at the wall in the initial section of the jet; $\bar{Q}$, excess heat content; $C = (T_0 - T_\infty)/(T_W - T_\infty)$, dimensionless excess fluid temperature at the exit from the slot (case C).

LITERATURE CITED

1. L. A. Vulis and V. P. Kashkarov, Theory of a Viscous Fluid Jet [in Russian], Nauka, Moscow (1965).
2. B. P. Beloglazov, Dokl. Akad. Nauk SSSR, 198, No. 3 (1971).
3. A. Angeaux, Mathematics for Electrical and Radio Engineers [Russian translation], Nauka, Moscow (1964).
4. B. P. Beloglazov and A. S. Ginevskii, Uch. Zap. Tsentr. Aéro-gidrodinam. Inst., 5, No. 4 (1974).

DIFFUSION IN A LAMINAR BOUNDARY LAYER OF A TURBULENT JET INCIDENT ON A PLATE

G. S. Antonova

UDC 532.522.2:532.7

Solutions are found for the stationary and nonstationary equations of convective diffusion on the basis of an experimentally detected hydrodynamic flow picture of an ideal fluid. The agreement between the results of boundary-layer soundings, obtained by different methods, is shown.

The requirements of practice evoked the necessity to investigate the process of metal surface dissolution under the effect of axisymmetric turbulent jets of aqueous solutions flowing perpendicularly into the surface. In particular, such a method of dissolving a metal surface is used in the production of electrical circuits for electronic apparatus.

The process of dissolving copper under these conditions is characterized by the constant delivery of a mass of solution to the surface, whereupon a heterogeneous reaction occurs on

Translated from Inzhenerno-Fizicheskii Zhurnal, Vol. 32, No. 4, pp. 674-682, April, 1977. Original article submitted April 13, 1976.